Effect of interface states on the performance of GaAs p^+-i far-infrared detectors

A. G. U. Perera, W. Z. Shen, and M. Ershov
Department of Physics and Astronomy, Georgia State University, Atlanta, Georgia 30303

H. C. Liu and M. Buchanan
Institute for Microstructural Sciences, National Research Council, Ottawa K1A 0R6, Canada

S. D. Gunapala, S. V. Bandara, and J. K. Liu
Center for Space Microelectronics Technology, Jet Propulsion Laboratory, California Institute of Technology, Pasadena, California 91109

H. H. Ye and W. J. Schaff
School of Electrical Engineering, Cornell University, Ithaca, New York 14853

(Received 13 August 1999; accepted 2 November 1999)

Interface states have been shown to have an appreciable effect on the performance of p-GaAs multilayer (p^+-i-p^+-i-...) homojunction interfacial work function internal photoemission (HIWIP) far-infrared detectors. In this article, a comparison of detector performance was made of p-GaAs HIWIP detectors with different interface state densities, with the emphasis on the detector's dark current, noise, and capacitance characteristics. © *2000 American Vacuum Society.* [S0734-2101(00)03502-8]

I. INTRODUCTION

Far-infrared range (40–1000 μm) is the source of much of the astrophysics information. The molecular and atomic emission lines associated with important species such as C, O, and H_2O are within this wavelength range. Dust, which is present both around and between stars, absorbs higher energy photons, also causing stars and galaxies to emit significant radiation in the infrared. Therefore, high performance far-infrared semiconductor detectors as well as focal plane arrays (FPAs) are in very high demand for space astronomy applications,[1] such as NASA's Stratospheric Observatory for Infrared Astronomy (SOFIA) and the ESA's far-infrared and sub-mm telescope (FIRST), for studying interacting galaxies, star formation and composition, and interstellar clouds. Recent development in the crystalline quality of semiconductor material and the fabrication technology has produced much progress in the far-infrared detectors. Blocked impurity band (BIB) detectors represent a significant advance in the state of the art of high performance detectors for far-infrared region. However, there are many technological challenges for fabricating larger format arrays in germanium,[2] and the detector wavelength coverage is limited by the energy of the direct ionization of shallow dopants in semiconductors, e.g., Si up to 40 μm, Ge up to 220 μm, and GaAs up to 300 μm.

Recently a novel Si or GaAs homojunction interfacial work function internal photoemission (HIWIP) far-infrared detector concept was proposed[3] and demonstrated[4,5] using molecular beam epitaxy (MBE) grown p^+-i multilayer structures. In addition to the advantage of the mature and uniform Si and GaAs material growth and monolithic integration technology, one of the unique features[3] is that in principle, there is no restriction on the cutoff wavelength (λ_c), which is tailorable, since the work function (Δ) can become arbitrary small with increasing doping concentration. Figure 1 shows the calculated doping concentration (N_a) dependence of λ_c from the high density theory[6] for p-GaAs, as well as the experimental λ_c obtained from p-GaAs HIWIP detectors. One important requirement in an array is an adequate detector-to-detector uniformity, acceptable operating temperature, and compatibility with different manufacturing processes. In this article, a comparison is made on two p-GaAs HIWIP FIR detectors grown and fabricated at different companies and the effect of interface states on the detector's dark current, noise, and capacitance characteristics is shown.

II. EXPERIMENT

The comparison was made of two typical MBE grown p-GaAs FIR HIWIP detector samples grown and processed

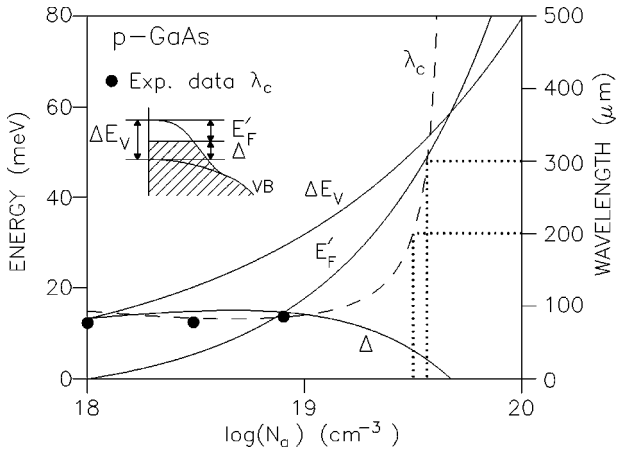

FIG. 1. Doping concentration (N_a) dependence of the shift for the valence band edge ΔE_v, interfacial work function Δ, and λ_c at zero bias calculated from the high density theory for p-GaAs at low temperature. The experimental λ_c obtained from p-GaAs HIWIP detectors are shown by solid circles. The dotted lines indicate concentration (3.2×10^{19} and 3.6×10^{19} cm^{-3}) needed to obtain $\lambda_c=200$ and 300 μm, respectively, at low bias.

TABLE I. Device parameters for the detector structures. Here, N is the number of multilayers, W_i, W_e, W_t, and W_b are the thicknesses of intrinsic (i), emitter (p^+), top and bottom contact (p^{++}) layers, respectively.

Sample No.	N	W_i (Å)	W_e (Å)	W_t (Å)	W_b (Å)
9604	20	800	150	3000	3000
G1-3A	10	800	150	1000	7000

by different institutes. Sample 9604 was grown by Cornell University and processed by National Research Council, Canada, and G1-3A was grown by Quantum Epitaxial Designs (QED), Inc. and processed by Jet Propulsion Laboratory (JPL). Table I shows their MBE epilayer parameters. The emitter layers were doped with Be which has an ionization energy of 28 meV in p-GaAs. The doping concentration is $4.0\times10^{18}\,\mathrm{cm}^{-3}$ for 9604 and $2.0\times10^{19}\,\mathrm{cm}^{-3}$ for G1-3A. The top and bottom contact layers were doped to $(2-3)\times10^{19}\,\mathrm{cm}^{-3}$, far above the Mott transition value to ensure an ohmic contact. Figure 2 shows the schematic of the detector after device processing and their energy-band diagram. Good control of MBE growth is indicated by secondary ion mass spectroscopy (SIMS) measurements.

III. DARK CURRENT CHARACTERISTICS

The present GaAs homojunction FIR detectors display symmetric dark current–voltage ($I-V$) characteristics due to the uniform doping in the emitter layers. Figure 3(a) shows the experimental dark current (dashed curve) at 4.2 K under positive biases for samples 9604 and G1-3A converted to the same device area of $1\times10^{-3}\,\mathrm{cm}^2$. The dark current in HIWIP detectors can be modeled by assuming a uniform electric field in the multilayers, and thermodynamic carrier equilibrium.[7] The dark current is the sum of the space-charge-limited (SCL) current, thermionic emission (TE) current, and tunneling current, and as a good approximation, the SCL current, TE current, and tunneling current can be treated separately.[7] Figure 3(a) also shows the calculated dark current (solid curves) for these two detectors with a hole scattering length of 300 Å.

The thermionic field emission (TFE) current was found to be the major source of dark current in these p-GaAs HIWIP detectors at 4.2 K. The increase in dark current in G1-3A with increased doping is expected as a result of modification to the Fermi–Dirac distribution. However, the dark current observed in 9604 sample was much higher than the values predicted according to the model. This deviation has been attributed to the existence of interface defect states.[7] The origin of these defect states can be the dangling bonds in the interfaces, Coulomb potential of charged ions, and impurities near interfaces. The existence of interface defect states can result in recombination via the defect states and generate currents. The G1-3A sample dark current has much better agreement with the model [less deviation as seen in the Fig. 3(a)] due to the better quality of material. A plot R_0A (R_0 is the dynamic resistance, and A is the device area) versus A for the 9604 sample showed a sharp drop (slope of 8.5 $\times10^3\,\Omega$) indicating leakage. In contrast, the G1-3A sample showed much improved (almost constant) R_0A values indicating much better quality material. Further evidence of this leakage can be seen from the relation of the dark current with the mesa area. As shown in Fig. 3(b), the 9604 sample displayed a superlinear (slope=1.62) increase with the mesa area, while the G1-3A displayed almost linear relation (slope=0.95).

IV. NOISE CHARACTERISTICS

The noise characteristics of the HIWIP detectors were measured using a low noise preamplifier (SR 560) and a fast Fourier transform (FFT) spectrum analyzer (SR 780) with the detector temperature at 4.2 K. The equipment was calibrated by measuring the room temperature noise level of a conventional 4.6 kΩ resistor. Typical current noise spectra of the studied 9604 and G1-3A p-GaAs HIWIP FIR detectors at 4.2 K under similar electric fields are presented in Fig. 4. Similar noise behavior was observed under reverse bias conditions. Also observed is the symmetry in dark current noise under forward and reverse biases due to the symmetric $I-V$ characteristics in HIWIP detectors.[8] In 9604 sample, the noise spectra display $1/f$ noise dependence at frequencies (f) below 1 kHz and are independent of frequency at higher values, while in G1-3A sample the noise spectra do not show $1/f$ noise and are independent of frequency over the whole range of measured frequencies.

In 9604, at low frequencies ($f\leqslant 1\,\mathrm{kHz}$), the $1/f$ noise power density is found[9] to be proportional to dark current I_d^{α} with an α value of 2.05–2.10. This type of behavior indicates that the origin of the $1/f$ noise in 9604 could be interpreted in

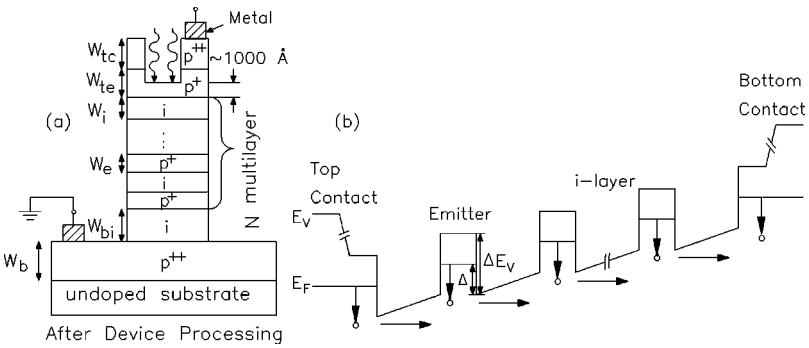

FIG. 2. (a) Schematic of the multilayer p-GaAs HIWIP detectors after device processing. p^{++}, p^+, and i are the contact layer, emitter layer, and undoped layer, respectively. A window is opened on the top side for frontside illumination. (b) Energy-band diagram of the detectors under forward bias.

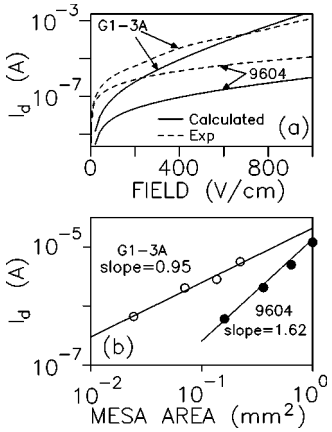

FIG. 3. (a). Experimental dark current at 4.2 K for samples 9604 and G1-3A (dashed curves) converted to mesa area of $1\times10^{-3}\,\mathrm{cm}^2$. The solid curves are the calculated dark current with a hole scattering length of 300 Å. (b) The mesa area dependence of dark current of the two samples at an electric field of 300 V/cm and its regression slope.

terms of a random fluctuation in the occupancy of the interface trap centers which can lead to generation–recombination (G–R) $1/f$ noise.[9,10] Based on this, the interface state density in 9604 have been estimated[11] from the noise power density in the order of $10^{11}\,\mathrm{cm}^{-2}$, a value which compared favorably with the density of interface states ($2.5\times10^{11}\,\mathrm{cm}^{-2}$) reported for MBE grown Be-doped p-type GaAs.[12] The experimental fact that no $1/f$ noise observed in G1-3A at low frequencies is a strong evidence of lower interface states, which is in agreement with the reduced deviation of the above dark current results.

The better material quality of G1-3A is also shown by its lower noise density throughout the measured frequency. The noise equivalent power (NEP) is proportional to the square root of the measured noise density at higher frequencies. At a frequency of 1500 Hz, the measured shot noise S_i is $5.10\times10^{-26}\,\mathrm{A}^2/\mathrm{Hz}$ in 9604, and $2.35\times10^{-26}\,\mathrm{A}^2/\mathrm{Hz}$ in G1-3A. This result shows the NEP would be 1.5 times lower in G1-3A sample.

V. CAPACITANCE CHARACTERISTICS

The bias and frequency dependent capacitance was measured using a computer-controlled Hewlett-Packard 4284A

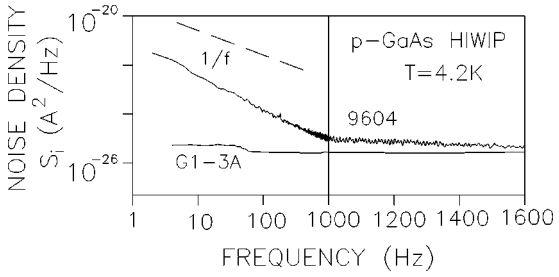

FIG. 4. Measured dark current noise spectra of p-GaAs 9604 (electric field of 300 V/cm) and G1-3A (electric field 250 V/cm) of HIWIP far-infrared detectors at 4.2 K. The dashed line represents the $1/f$ dependence of the noise power density S_i.

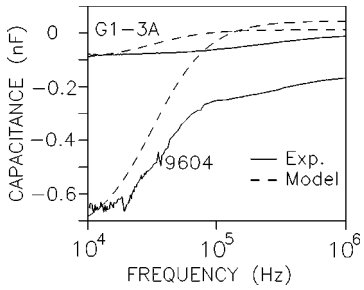

FIG. 5. Experimental frequency dependence of capacitance in 9604 and G1-3A at 4.2 K under an electric field of 1800 V/cm. The dashed curves are the calculated capacitance-frequency characteristics.

LCR meter. The modulation voltage did not exceed 5.0 mV, which is much less than the barrier heights at interfaces between the emitter and intrinsic layers. The capacitance displays a maximum at zero bias, decreases rapidly with increasing bias voltage, and reaches negative values at higher biases. The decrease is more rapid at low frequencies. The capacitance at zero bias decreases with frequency, approaching the value of the geometric capacitance at high frequencies. Figure 5 shows the experimental frequency dependence of capacitance (solid curves) for samples 9604 and G1-3A at 4.2 K under similar electric fields. The capacitance at lower biases is positive at higher frequencies and decreases with frequency to negative values. However, at higher biases, as shown in Fig. 5, the capacitance is negative in the whole frequency range measured and decreases rapidly with the frequency, where the absolute value of the negative capacitance at low frequencies can be much higher than the geometric capacitance.

The negative capacitance phenomenon in HIWIP detectors has been attributed[11] to the carrier capture and emission from the interface states. In the presence of an alternating-current (ac) perturbation with a small voltage δV, the interface traps can retain a sufficient quantity of charge so that they build a dipole layer which modulates the barrier height. The variation of barrier height δV_i arises mainly from carrier capture and emission at interface states. This process requires a certain period of time, which makes δV_i (and dark current) lag behind δV. Since lower interface states have been observed in G1-3A (from the dark current and noise measurements), weaker negative capacitance phenomenon is expected in G1-3A, as clearly shown in Fig. 5.

A fitting model based on charging-discharging current and the inertial conducting current shows good agreement with the experimental observations,[11] and the frequency (ω) dependence of the capacitance $C(\omega)$ can be written as

$$C(\omega)=C_0-\frac{\Delta G_i\tau-\Delta C_i}{1+(\omega\tau)^2}, \tag{1}$$

where C_0 is the geometric capacitance, ΔG_i is the variation of conductance, τ is a time constant of the interface trap characterizing the current relaxation time, and ΔC_i is the capacitance variation, which is determined by the interface trap's concentration, activation energy, and band bending. Figure 5 also shows the simulation results (dashed curves) of

the capacitance-frequency characteristics at 4.2 K for 9604 and G1-3A. The parameters were estimated from the following consideration. C_0 is 44 pF for 9604 and 12 pF for G1-3A from the parallel plate approximation for geometric capacitance. ΔG_i ($1.0\times10^{-3}\,\Omega^{-1}$ for 9604 and $6.2\times10^{-4}\ \Omega^{-1}$ for G1-3A) is estimated from the detector's differential dark current results at 4.2 K. τ is selected to be 5.0 μs, since the relaxation time of transients has normally a few μs.[13] As indicated before, ΔC_i is the most important parameter related to the interface states, which should increase rapidly with the interface state density. A reasonable qualitative agreement of the fitting results and experimental data is observed by using ΔC_i of 4200 pF for 9604 and 200 pF for G1-3A. This result strongly supports the conclusion of lower interface states in G1-3A. The calculated detector capacitance at low frequency is sensitive to ΔC_i, since ΔG_i keeps constant at a fixed bias. The deviation of the simulation from the experiments at high frequencies is mainly due to the neglect of frequency dependent behavior of ΔG_i and ΔC_i in the simulation.

VI. CONCLUSION

In summary, a comparison study has been made on *p*-GaAs HIWIP FIR detectors grown and fabricated at different companies. The emphasis is on the detector's dark current, low frequency noise, and negative capacitance characteristics. Interface states have been shown to have an appreciable effect on the detector's performance.

ACKNOWLEDGMENTS

This work was supported in part by the National Aeronautics and Space Administration under Contract No. NAG5-4950. The authors wish to acknowledge Dr. S. G. Matsik and Dr. A. Korotkov at GSU for their technical help.

[1]M. W. Werner, Infrared Phys. Technol. **35**, 539 (1994).
[2]E. E. Haller, Infrared Phys. **35**, 127 (1994).
[3]A. G. U. Perera, H. X. Yuan, and M. H. Francombe, J. Appl. Phys. **77**, 915 (1995).
[4]A. G. U. Perera, W. Z. Shen, H. C. Liu, M. Buchanan, M. O. Tanner, and K. L. Wang, Appl. Phys. Lett. **72**, 2307 (1998).
[5]W. Z. Shen, A. G. U. Perera, H. C. Liu, M. Buchanan, and W. J. Schaff, Appl. Phys. Lett. **71**, 2677 (1997).
[6]S. C. Jain and D. J. Roulston, Solid-State Electron. **34**, 453 (1991).
[7]W. Z. Shen, A. G. U. Perera, M. H. Francombe, H. C. Liu, M. Buchanan, and W. J. Schaff, IEEE Trans. Electron Devices **45**, 1671 (1998).
[8]A. G. U. Perera, H. X. Yuan, S. K. Gamage, W. Z. Shen, M. H. Francombe, H. C. Liu, M. Buchanan, and W. J. Schaff, J. Appl. Phys. **81**, 3316 (1997).
[9]W. Z. Shen and A. G. U. Perera, IEEE Trans. Electron Devices **46**, 811 (1999).
[10]O. Jantsch, IEEE Trans. Electron Devices **34**, 1100 (1987).
[11]A. G. U. Perera, W. Z. Shen, M. Ershov, H. C. Liu, M. Buchanan, and W. J. Schaff, Appl. Phys. Lett. **74**, 3167 (1999).
[12]J. Qiu, Q. D. Qian, R. L. Gunshor, M. Kobayashi, D. R. Menke, D. Li, and N. Otsuka, Appl. Phys. Lett. **56**, 1272 (1990).
[13]M. Ershov, H. C. Liu, L. Li, M. Buchanan, Z. R. Wasilewski, and A. K. Jonscher, IEEE Trans. Electron Devices **45**, 2196 (1998).